Errata Sheet

SEMI-ANNUAL PROGRESS REPORT NO. 15
Task Order No. EDG-4

1. In Figure 5, Page 9 - Remove the link joining the grid and cathode of the first tube.

2. On Page 29 Line 8 - Change $L^{-1/2}$ to $\frac{1}{2\pi} L^{-1/2}$.

ENGINEERING RESEARCH INSTITUTE
UNIVERSITY OF MICHIGAN
ANN ARBOR

WIDE-RANGE TUNING METHODS AND TECHNIQUES

APPLICABLE TO SEARCH RECEIVERS

SEMI-ANNUAL PROGRESS REPORT NO. 15, TASK ORDER NO. EDG-4
Period Covering January 1, 1955 to June 30, 1955

Electronic Defense Group
Department of Electrical Engineering

By: L. W. Orr
T. W. Butler, Jr.
H. Diamond
K. Grabowski
M. Winsnes

Approved by: H. W. Welch, Jr.

Project 2262

CONTRACT NO. DA-36-039 sc-63203
SIGNAL CORPS, DEPARTMENT OF THE ARMY
DEPARTMENT OF ARMY PROJECT NO. 3-99-04-042
SIGNAL CORPS PROJECT 194B

July, 1955

TABLE OF CONTENTS

LIST OF ILLUSTRATIONS

ABSTRACT

The progress of the Electronic Defense Group on Task EDG-4 is reviewed for the first half of 1955. The equipment for carrying out spot check measurements on ferrite cores is now complete. Modifications of the Blare equipment have been made which permits automatic recording of Butterfly loops for magnetic toroids. Silver electrodes have been successfully deposited on ceramic samples and preliminary measurements are being carried out on ceramic samples with gold electrodes. Vacuum-evaporated coatings are also being applied to ferrite samples made by EDG-Task 6. High frequency Q measurements have begun on ferro-electric capacitors with variable d.c. field and data are reported in the form of a Q.E.F. surface. Considerable progress has been made in the technique used in constructing microcaps. Life testing equipment has been constructed and a schedule has been established to obtain life test data on microcaps under conditions closely approximating those in tuning applications. A study is presently being carried out to determine the feasibility of using silicon junction diodes as a means of electric tuning. An investigation is being made for the use of ferroelectric capacitors in voltage-tunable power oscillators. Measurements of noise figure, image signal interference and oscillator 2nd harmonic interference effects have been made on Pandu front end assemblies. New front end assemblies are being constructed featuring low noise figures, single voltage tracking, band spread and linearized sweep frequency. The objectives for the period have been accomplished.

WIDE RANGE TUNING METHODS AND TECHNIQUES APPLICABLE TO SEARCH RECEIVERS

SEMI-ANNUAL PROGRESS REPORT NO. 15, TASK ORDER NO. EDG-4

Period Covering January 1, 1955 to June 30, 1955

1. PURPOSE

This report reviews the progress made by the Electronic Defense Group in the study of wide range tuning methods and techniques applicable to search receivers during the first half of 1955.

2. PUBLICATIONS AND REPORTS

Mr. H. Diamond attended the "Symposium of Ferroelectricity" at the Hexagon, Fort Monmouth, N. J. on January 26, 1955.

Mr. H. Diamond attended the Toronto meeting of the American Physical Society, June 22 to 24, 1955.

Dr. L. W. Orr and Mr. T. W. Butler, Jr. consulted with Mr. A. Rodrigues, Chief Engineer of the Engineering Research Department of the Aerovox Hi-Q Division in Franklinville, N. Y. on June 27, 1955.

3. FACTUAL DATA

3.1 Ferromagnetic Materials (M. Winsnes and L. W. Orr)

3.1.1 SCF Measurements on Ferrite Cores. Spot check with field (SCF) measurements on ferrite cores are being made with the equipment shown in Figure 1.

FIG. 1

SCF EQUIPMENT

This equipment is now complete. This equipment provides a fast method of measuring μ and Q of ferrite toroids as a function of dc bias field at a fixed frequency. The inductance, L_1 in this figure, serving as the decoupling impedance between the dc source and the toroid, has been replaced by a parallel resonant circuit to give the maximum possible rf impedance at 500 kc., which is the Q-meter frequency used in the tests to date.

To obtain the actual Q of the toroid core, the observed data have to be corrected for the effects of copper loss in the winding, contact resistance of the small plugs, and the loading effect of the decoupling impedance. To facilitate this reduction of the Q data, correction charts have been drawn.

The results of a series of measurements on ferrite cores made by EDG Task 6 are shown by the μ-Q plots[1] in Figure 2. The μ values for zero field are indicated by the highest points on each curve. As the dc field is applied, μ decreases. The lowest points on the curves correspond to a dc field of 30 oersteds.

The quality factor for a ferrite is generally expressed as the μQ product. The curves in Figure 2 indicate that in general this product decreases with the application of dc field, but this is not generally true for all classes of ferrites. The maximum μQ product was obtained with the E-101 core at zero field, having a value of about 23,000.

3.1.2 Transverse μ and Q Measurements. The transverse permeability, μ_t, and associated Q_t, imply a bias field at right angles to the direction of the rf measuring field. To obtain μ_t and Q_t data on ferrite toroids, an electro-

[1] These plots are discussed in more detail in Electronic Defense Group Technical Report No. 48, "A Graphical Presentation of Some Ferrite Characteristics", by M. Winsnes, P. Nace and D. Grimes, University of Michigan, April 1955.

2262 A-66-129 AEM 7-20-55

FIG. 2

μ - Q WITH PARALLEL D.C. BIAS (500 KC)

2262 A-66-128 AEM 7-20-55

FIG. 3

μ - Q WITH TRANSVERSE D.C. BIAS (500 KC)

magnet is used with the toroid placed between the poles. The toroid axis is placed parallel to the axis of the electromagnet. This is accomplished by making one pole of the electromagnet moveable, and separating the toroidal inductor from the poles with 1/8 inch lucite spacers. The toroid is carefully wound with a single layer of wire having no wires crossed to insure parallelism of the finished faces. This winding can be directly connected to the Q meter, and no isolating impedance is required for these measurements since the field is furnished external to the toroid.

The results of the tests on the same cores as in Figure 2 are shown by the μ-Q plots in Figure 3 for 500 kc. The maximum field (point of lowest μ) was in each case somewhat in excess of 30 oersteds transverse field. The actual field is difficult to determine because of the field distortion between the poles of the electromagnet, due to the presence of the specimen, and the variation in this distortion as the permeability of the specimen varies. It is interesting to note that the transverse Q's are generally larger than the corresponding parallel Q's.

The transverse μ and Q data were obtained for the 5 cores shown in Figure 3 at a number of different frequencies. Figure 4 shows a typical set of curves for one of the cores. This indicates a general decrease in the μQ product at all values of dc field as the frequency is increased from 0.5 to 10 mc.

3.1.3 Q-Meter Accessories. Since some of the Q readings are quite low, a more sensitive method of measuring the Q than that provided by the Boonton 160 Q-meter alone was needed. For frequencies up to 2 mc, a Hewlett-Packard Model 400-C VTVM was connected across the tuning capacitor of the Q-meter. This permitted measurement of Q's down to unity. The added capacity of the VTVM can easily be taken into account.

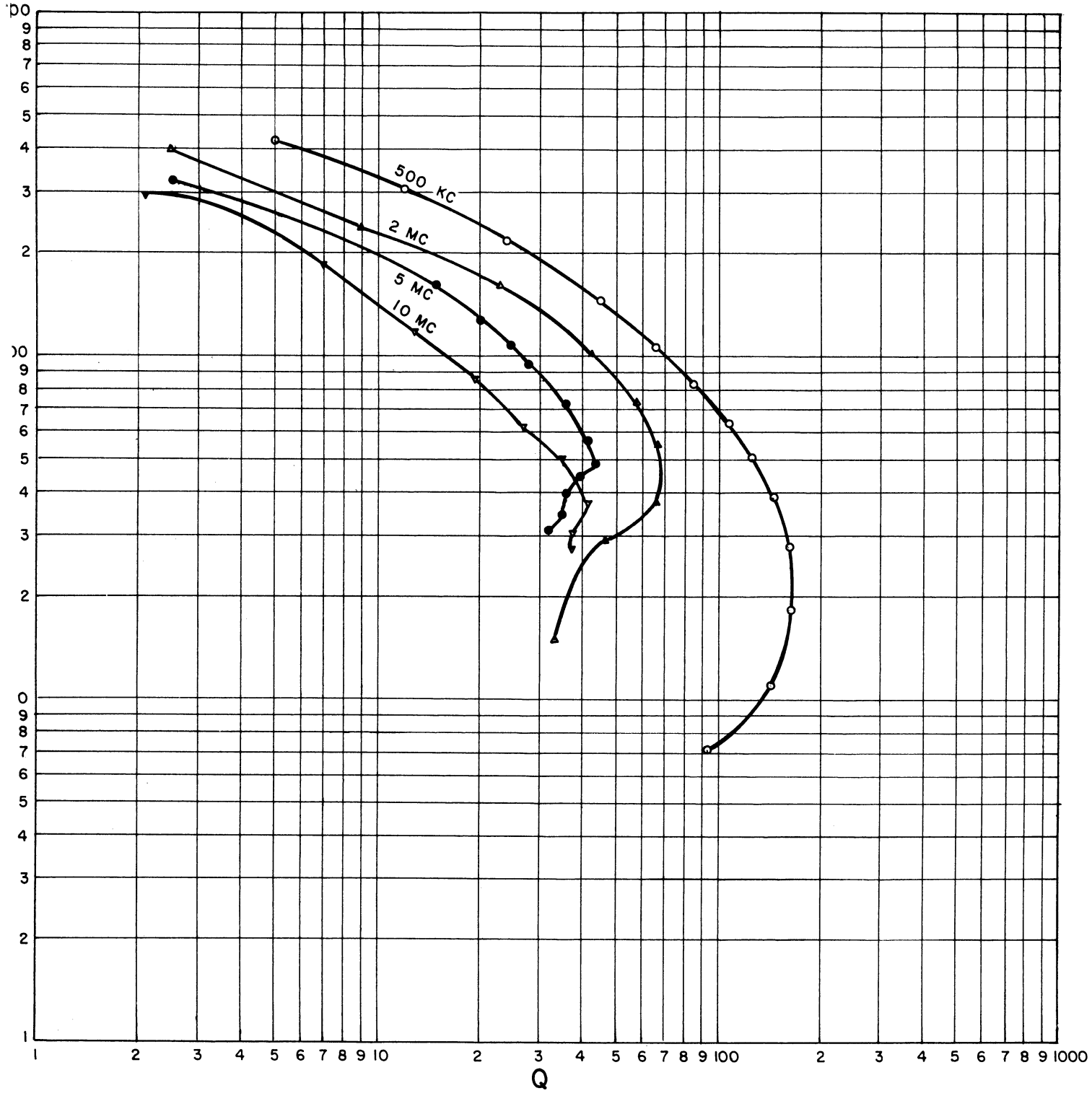

FIG. 4

μ-Q WITH TRANSVERSE D.C. BIAS FOR A-105-1

For frequencies above 2 mc, it was necessary to use a Hewlett-Packard Model 410-B VTVM to obtain the required frequency response. However, because of the lower sensitivity of this meter, a preamplifier was necessary. The circuit of the preamplifier is shown in Figure 5. This circuit gives a voltage gain of 10, and is flat within one db between 0.1 and 40 mc. It has an input impedance of 10 megohms shunted with 9 μμf.

By using the Model 410-B with this preamplifier, it was possible to measure Q's down to unity with good accuracy. This setup was used for the high frequency data shown in Figure 4.

3.1.4 BLARE Modifications. A modification of the BLARE equipment[1] has been made which permits automatic recording of Butterfly loops for magnetic toroids. The magnetic butterfly loop is a plot of μ vs. H, when H is cycled slowly and symmetrically about zero.

Figure 6 shows the circuit of the variable dc current supply and the method of connecting the ferrite toroidal inductor. The supply gives a maximum current of 2 amperes, and the slow variation is obtained by means of a temperature-limited diode (actually, four 5U4 rectifiers). The diode is furnished with a varying heater power by means of the BLARE motor-controlled variac and a suitable step-down transformer. The source of dc current through the diode is furnished by a separate supply.

As the dc current is slowly varied through the inductor, a steady 1000 cycle current is also applied. The ac voltage developed across the inductor is proportional to its impedance and is therefore a measure of the permeability of the core. This voltage is therefore fed to the BLARE amplifier and detector, and finally to the pen input of the recorder. The drum input of the recorder is

[1] The BLARE equipment is discussed in more detail in Quarterly Progress Report No. 14, Task Order No. EDG-4, January 1955.

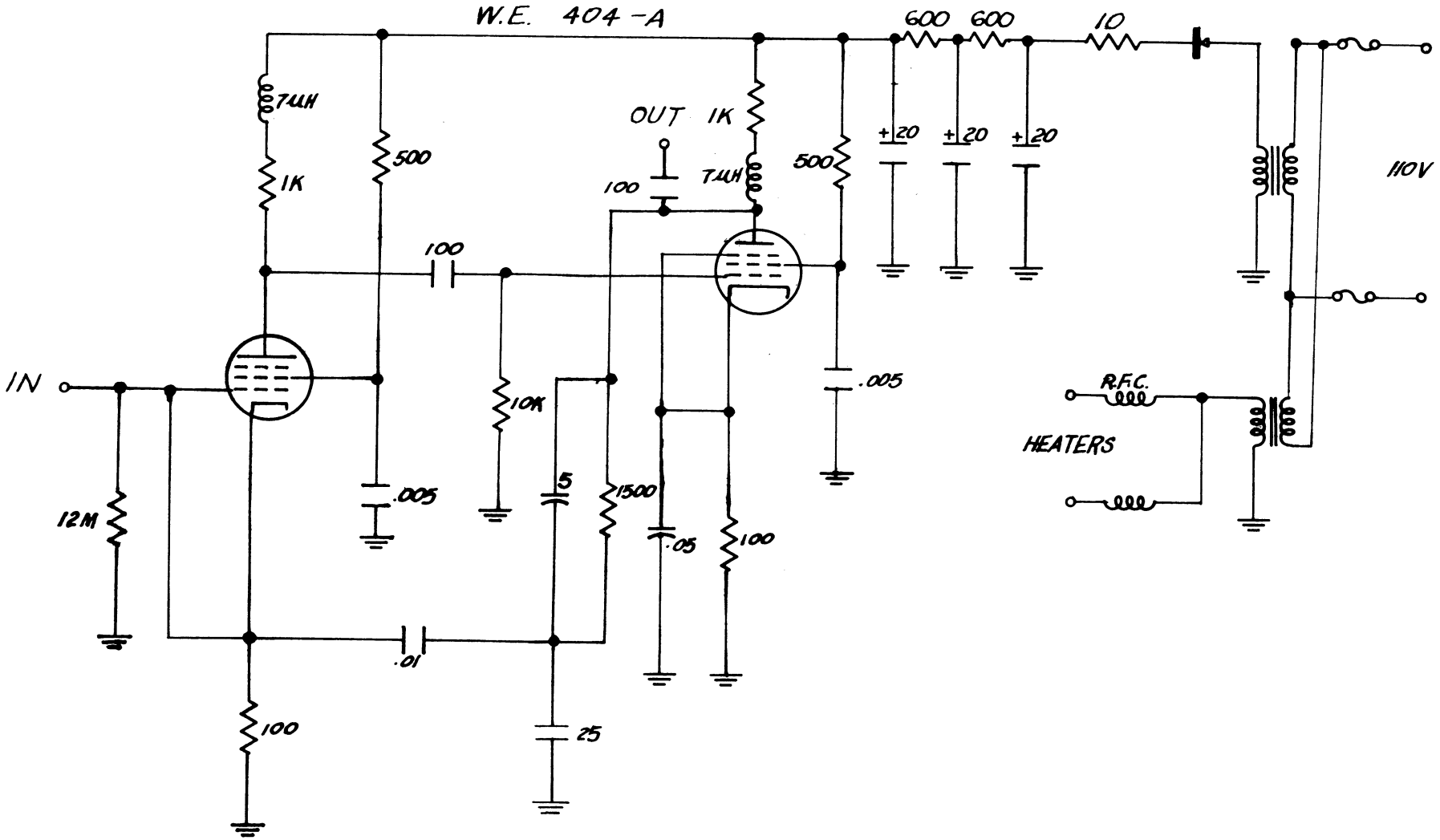

FIGURE 5
PRE AMPLIFIER FOR 410 B H.P. VTVM

A-CT-210 C.W. JUNE 11, 1955

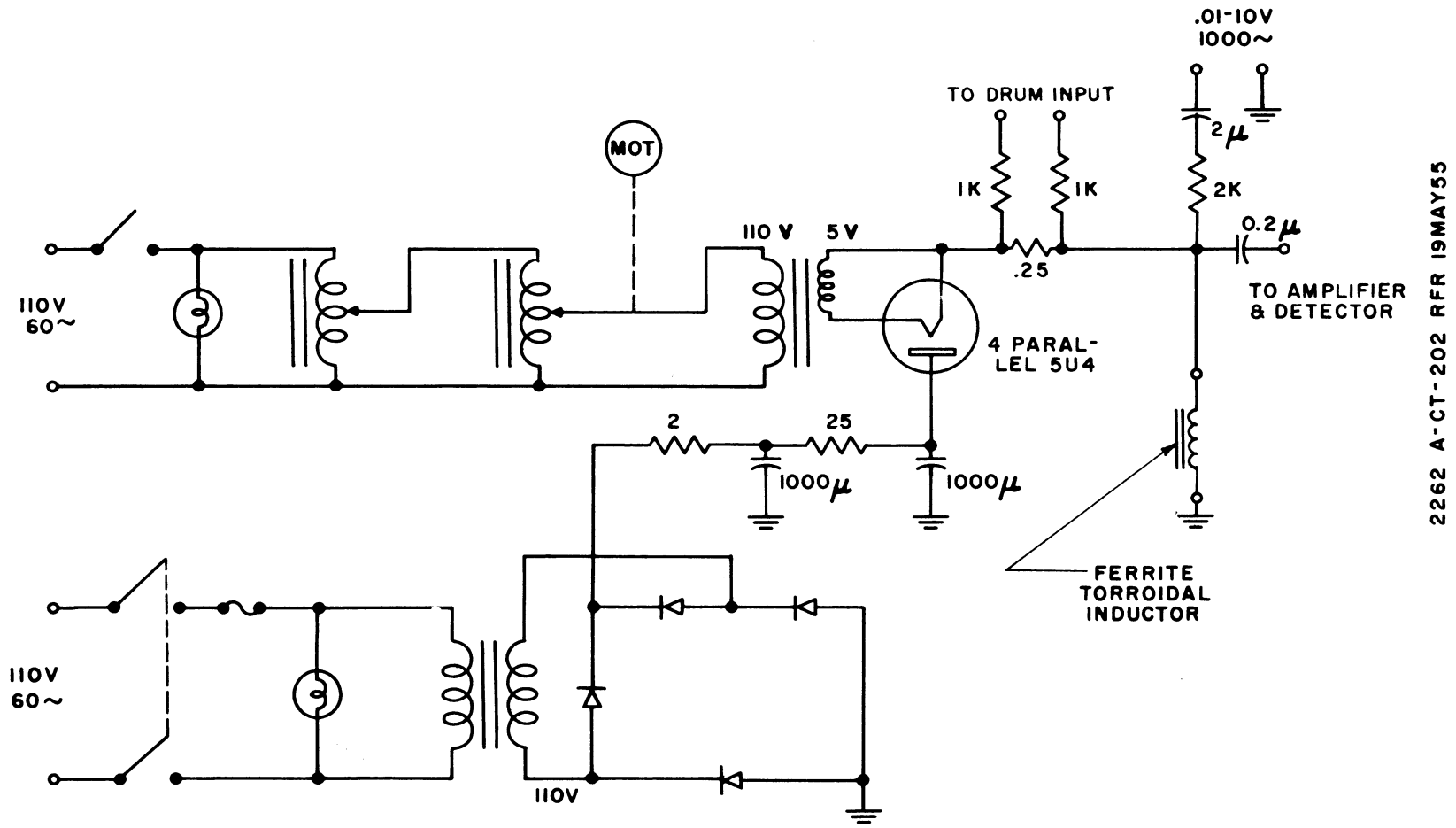

FIG. 6

VARIABLE CURRENT (0-2a) SUPPLY

obtained from the voltage drop across the 0.25 ohm resistor, this voltage being proportional to the applied dc field. The two 1K resistors are used for isolation purposes.

When the automatic features of BLARE are employed, one wing of the butterfly loop is obtained. To obtain the second wing of the loop, the inductor leads, and the drum input leads are reversed at times of zero dc current. A typical Butterfly loop for a ferrite toroid is shown in Figure 7.

3.2 Ferroelectric Materials (H. Diamond, K. Grabowski and L. W. Orr)

3.2.1 Vacuum-Evaporated Electrodes. During the period covered by this report, the high vacuum equipment has been installed and checked and is now working satisfactorily. Silver electrodes have been successfully deposited on ceramic samples, and, more recently, gold electrodes have been deposited. Gold electrodes have the advantage that they do not oxidize. This is based on single experimental samples exposed to air. However, thin gold electrodes do dissolve on soldering, and an electro-plating method is being considered in order to thicken the electrode. Preliminary measurements are now being made on ceramic samples with gold electrodes, but it is too early to report any results at this writing.

Vacuum-evaporated coatings are also being applied to ferrite samples made by EDG Task 6. This will facilitate resistivity measurements of various ferrite materials.

3.2.2 QEF Surfaces. The variation of Q of a ceramic capacitor when both the electric field and the frequency are varied is conveniently demonstrated by a three dimension plot called a QEF surface.[1] Considerable data have been

[1] See, for instance, Quarterly Progress Report No. 14, Task Order No. EDG-4, January 1955.

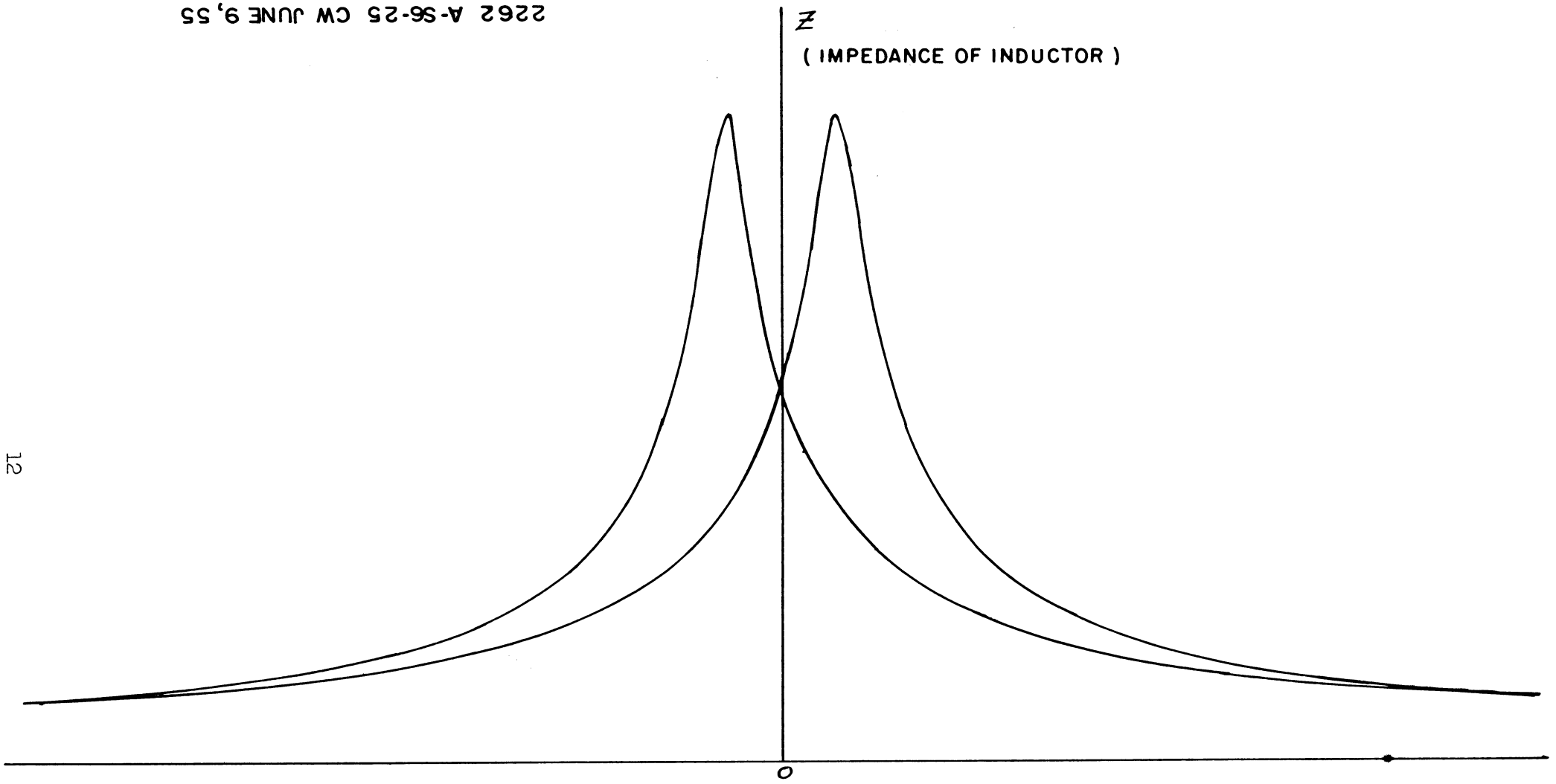

FIG. 7 BUTTERFLY - LOOP, 1000 CPS A-231-12

obtained on Aerovox Hi-Q 40 (which is the most suitable to date for tuning applications). Frequencies from 2 to 260 mc were used with fields varying from zero to 100 volts per mil. Upon application of a field, the Q appears to reach a peak at about 34 mc., as shown in Figure 8. In the range 5 to 35 mc, pronounced dips in Q are observed for even small fields, as shown in Figure 9. These dips are attributed to piezo-electric resonances in the ceramic sample. In the design of a tuning element, such regions of piezo-electric resonances must be avoided. The regions are depressed in frequency as the sample thickness is increased. This has not been experimentally determined. The frequency region from 0.2 to 2 mc is now being investigated.

3.2.3 Domain Relaxation Effects. No progress has been made in this area of investigation since the previous report, but the equipment is on hand and it is planned to continue this work in the near future.

3.2.4 Construction of Microcaps. Considerable progress has been made in the techniques used in constructing microcaps (sub-miniature capacitors) which are voltage sensitive, and therefore suitable for high frequency tuning applications. The method of construction differs from that previously described in that the material is diced into very small squares by means of a diamond cutting wheel. To support the ceramic during cutting, it is cemented to a microscope slide, which is then waxed onto a flat steel plate held in the magnetic surface clutch of the precision grinder. The uniform size of units made by this method is of great assistance in producing a batch of capacitors to tolerance specifications.

The chief cause of failure in microcaps is the presence of slight traces of moisture during potting. Leakage resistances greatly in excess of 100 megohms are required for satisfactory operation. Great care must be taken to

FIG. 8

Q-E-F SURFACE
AEROVOX HI-Q-40 FERROELECTRIC CERAMIC

2262 A-66-137 RRC 7-12-55

Q vs FREQUENCY
AEROVOX HI-Q-40 CERAMIC

FIG. 9

avoid the entrapment of moisture during the construction, and various techniques are being developed for this purpose. At present, thermosetting plastics are being investigated as alternative potting materials, and hermetic vacuum sealing techniques are being considered to improve reliability.

The P-E loop of a microcap degenerates rather severely with even relatively high leakage resistance. Figure 10a shows the 60 cycle P-E loop of a 100 μμf microcap which has approximately 100 megohms leakage resistance. Figure 10b shows the hysteresis loop for an acceptable capacitor.

More complete details regarding the construction and assembly techniques of microcaps will appear shortly in a technical report now in preparation.

It is expected that upon the further investigation of vacuum deposited electrodes, microcaps having smaller losses at high frequencies can be constructed. Previous experiments have shown thinner P-E loops with vacuum deposited electrodes than with Dupont silver paint electrodes which are common in commercial capacitors.

3.2.5 Life Tests on Microcaps. A life testing schedule has been established to obtain life-test data on microcaps under conditions closely approximating those in tuning applications. A testing unit has been constructed having the circuit shown in Figure 11. Units are subjected to combined dc and 60 cycle ac voltages. Component failure is indicated by neon glow lamps which remain dark normally, and glow when a unit has failed.

Life test data on the first samples of material are not available at this writing, but will be reported at a later date.

3.2.6 Ferroelectric Stacks. The ferroelectric stacks are multiple units consisting of alternate layers of sheet metal electrodes and ferroelectric ceramic squares. The metal electrodes extend well beyond the edges of the ceramic

(a)

(b)

FIG. 10

P-E AND HYSTERESIS LOOP
FOR A TYPICAL MICROCAP

FIG. 11

CAPACITOR LIFE TEST UNIT

to act as cooling fins. The ferroelectric stacks were constructed primarily for use in the voltage-tunable power oscillator work described in a later section of this report.

The form of the stack is shown in Figure 12, and was derived from the following considerations: (1) the rf voltage per capacitor unit should be as small as practicable, while the full value of the dc control voltage is applied to each unit; (2) dielectric heating should be kept small, and good heat dissipation be maintained so that the temperature does not rise excessively causing loss of tuning range, and possible thermal failure.

The stacks are constructed by tinning the ends of the electrode strips on both sides. The squares of ceramic, which have a commercial one mil silver coating on both sides, are then cut and the surfaces rubbed bright to help the solder to adhere. The stack is then assembled by successively sweating the component parts into place. Finally, a potting material is applied to prevent moisture absorption and surface breakdown.

3.2.7 Literature Survey. To keep abreast of various developments in the ferroelectric ceramic field, and to estimate the potentialities and limitations in this field, a continuing survey is being made of the literature.

3.2.8 BLARE Data on Ferroelectric Materials. During the past 6 months, a considerable volume of data has been obtained on various materials showing the variation of ϵ at 1000 cycles with variations of T and E. These data are most conveniently presented in the form of ϵ-T-E surfaces (formerly called epsilon-temperature surfaces). These surfaces are drawn in the form of charts, and it is anticipated that these charts will be published in a short technical report in the near future.

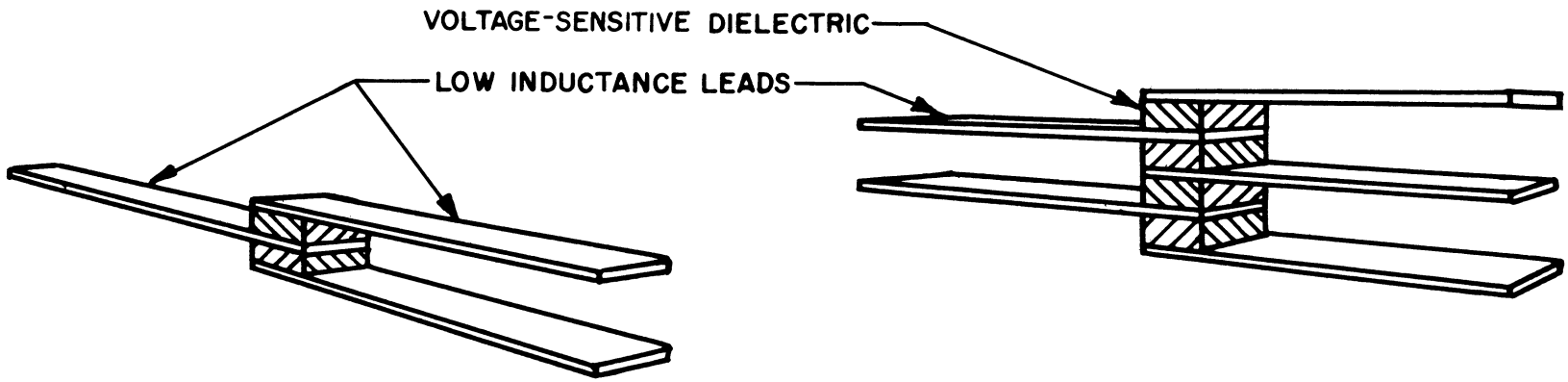

FIGURE 12

PHYSICAL ARRANGEMENT OF THE CAPACITOR STACK

3.3 Semiconductor Materials

3.3.1 Diode Tuning. Silicon junction diodes exhibit a variation of their effective shunt capacitance when polarized with a variable voltage in the non-conducting direction. This phenomenon has been suggested as a means of electric tuning, and a survey of commercially available types of diodes is being conducted. The results to date are summarized in Table 1.

TABLE 1

Type	Back Voltage	C in μμf	Q
Hughes HD-6002	0 60	5.3 2.27	15.2 34.8
Hughes HD-6001	0 60	18.0 5.1	31. 43.5
Transistor Prod TP 1N108	0.5 30.	39 11.5	2 21.6
Texas Insts TI 518	0 30	8.6 3.9	7.2 15.9

The data in Table 1 were obtained at 15 mc using a Boonton Model 160-A Q-meter. The Q data were obtained by reducing the actual Q readings to give the Q of the diode.

The change in capacitance and Q at 15 mc, with applied back voltage, is illustrated for a typical unit in Figure 13. It has been learned that the RCA Laboratories in Princeton, New Jersey are also working on this problem, and are constructing special diodes designed specifically for voltage-tuning to give improved performance.

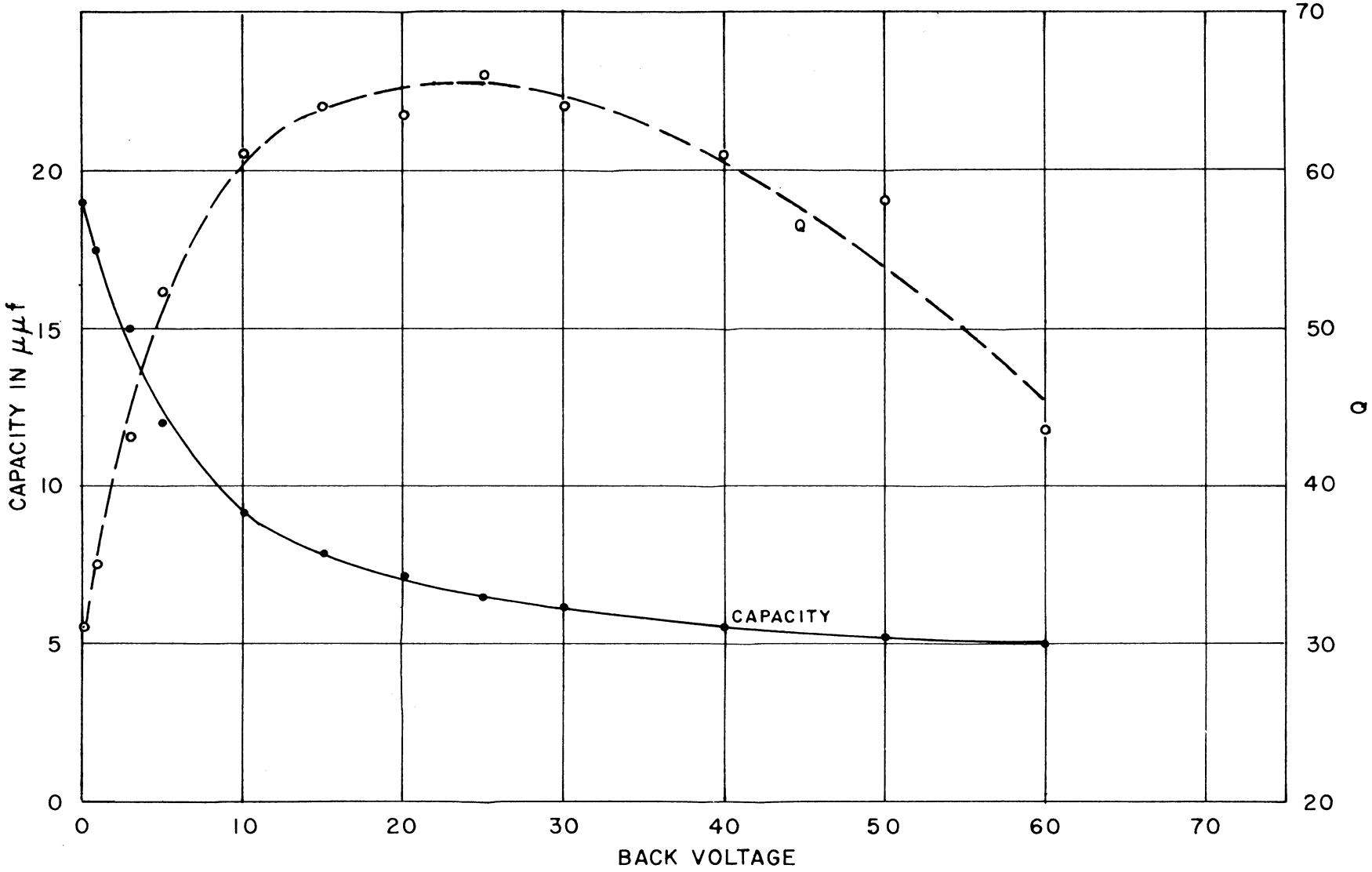

FIGURE 13

Q AND C VS. BACK VOLTAGE
DIODE HD 6001

2262 A-G4-107 AEM 7-6-55

3.4 Applications of Ferroelectric Materials (T. W. Butler, Jr., K. Grabowski and L. W. Orr)

3.4.1 Very High Frequency, Voltage-Tunable Oscillators. The maximum frequency achieved to date in a voltage-tunable oscillator using ferroelectric capacitors is still 385 mc as previously reported. However, this is not due to a limiting feature of the material, but to the fact that very little activity has occurred in this area for the past six months. With the development of improved production techniques in making microcaps, it is expected that this top frequency will be extended during the next interval.

3.4.2 Voltage-Tunable Power Oscillators. An investigation is being made of the use of ferroelectric capacitors in a voltage-tunable power oscillator. The tuning element is a capacitor stack constructed as described above in Section 3.2.6. The circuit showing the most success is given in Figure 14. This push-pull circuit proved to be superior to the other circuits used, which were single-ended Hartley, Colpitts and Ultra-audion circuits. The relatively low Q of the capacitor stack requires the push-pull circuit to obtain an adequate power output.

Capacitor stacks used were between 100 and 200 μμf, and the frequency used was in the range 40 to 100 mc. Output power was obtained by means of a coupling loop feeding a 10 ohm resistor. Power was measured by making voltage measurements across the 10 ohm resistor with a VTVM.

It was recognized that the capacitors must not be allowed to heat excessively because the capacitance range, and hence the tuning, is drastically reduced at temperatures much above the Curie point. To prevent excessive temperature rise, a strong jet of air was directed on the stack during operation.

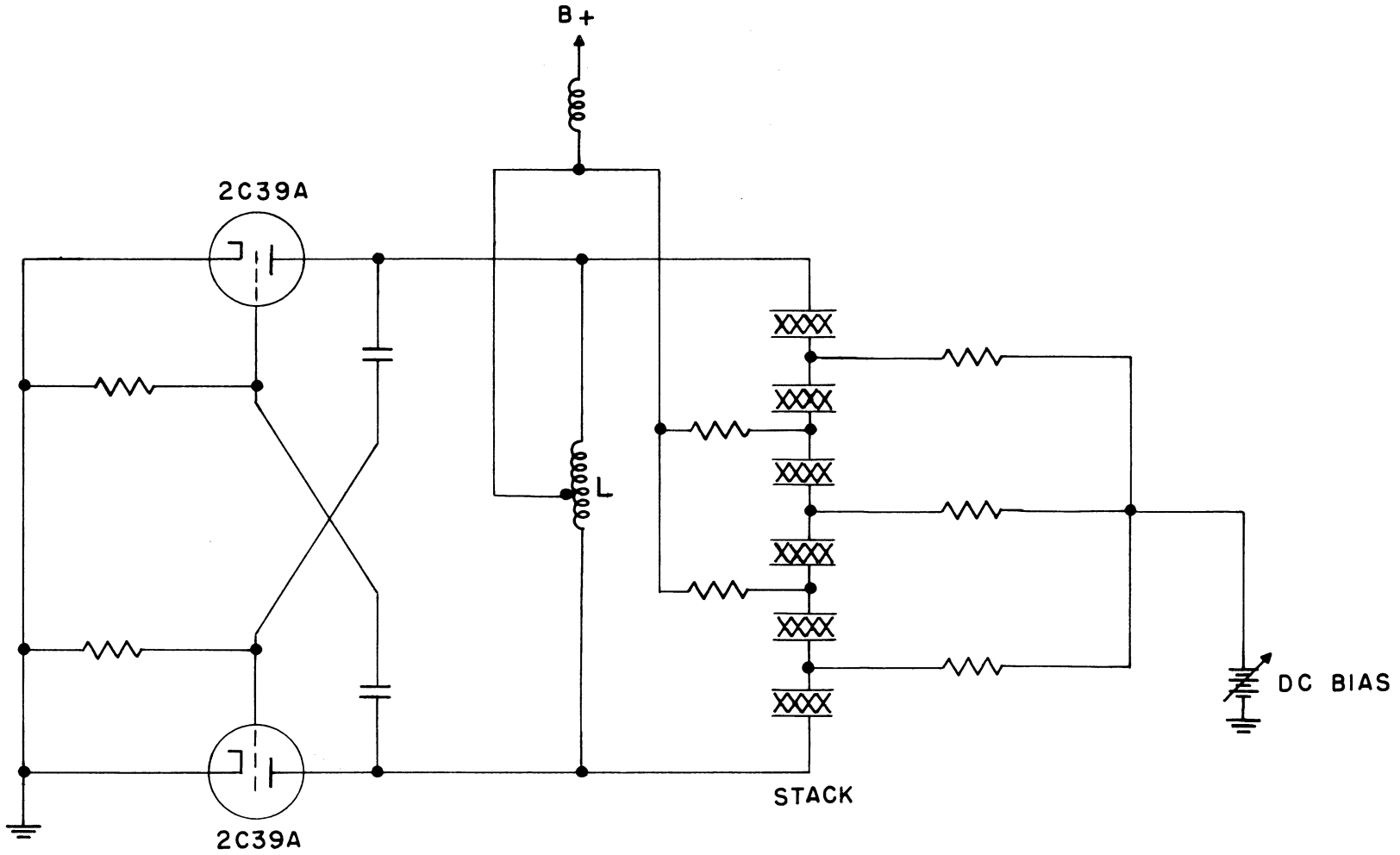

2262 A-CT-215 AEM 7-8-55

FIG. 14

VOLTAGE TUNABLE POWER OSCILLATORS

Two effects are noticed about the operation of the oscillator.

(1) At constant anode supply voltage there is an increase in output power, in addition to the increase in frequency, when the dc bias is applied. This is due to the increased Q of the capacitors at large dc field values.

(2) An increase in output power level, produced by raising the anode supply voltage, was found to reduce the tuning range in spite of the presence of the jet of cooling air. It was concluded that the jet of air does not provide adequate cooling for CW operation.

When the oscillator was operated at high power, but pulsed on a sufficiently small work cycle so that the capacitors remained relatively cool, the tuning range was about the same as for low power CW operation. This is illustrated by the curves in Figure 15. The power output was roughly 3 watts at the high power level, and about 100 mw at the low power level.

3.5 PANDU Program

3.5.1 Single Voltage Tracking. In previous Front End Assemblies, the RF amplifier, mixer, and local oscillator stages were tuned by varying the dc biases and amplitudes of the ac sweep with six independent adjustements to obtain the best tracking over the band. A new Front End unit is being constructed in which the same voltage will be fed to all three stages. If the capacitance of each tuned stage follows the law

$$C = C_o \cdot f(E) \qquad (1)$$

where the function, f(E), of applied voltage is the same for all voltage sensitive capacitors, tracking can be accomplished by using conventional tracking theory[1].

[1] See, for instance, Radio Receiver Design, Part I, by K. R. Sturley, 2nd Edition Revised, Chapman and Hall, 1953.

FIGURE 15

POWER OSCILLATOR TUNING CHARACTERISTICS

The local oscillator circuit will require the addition of a trimmer capacitor, C_t, and a padder capacitor, C_p, as shown in Figure 16. In addition, a dc return path to ground through R_1 (Figure 16) is required so that voltage sensitive capacitor C_1 will receive the full tuning voltage, E.

3.5.2 Bandspread. Using the system of single voltage tracking, the front end will be tracked over the whole band with a tracking error which is minimized. Any section of the band may now be used for bandspread, by the simple means of reducing the ac, or sweeping component of the tuning voltage, to an appropriate small value. The center frequency may be selected by a suitable adjustment of the dc component of the sweeping voltage. Because of the six independent voltage controls on previous PANDU heads, this method of bandspread could not be evaluated. However, with the head now in construction, it should be possible to evaluate bandspread using 2 controls.

3.5.3 Linearizing the Frequency Sweep. To give a linear frequency scale on the display scope, the shape of either the tuning voltage or of the voltage applied to the horizontal sweep may be altered. Since it is desired to have a linear frequency change with time, thus obtaining a uniform response rate, a linear sawtooth voltage will be used to drive the horizontal sweep of the scope. It is now necessary to derive the shape of the required tuning voltage to give linear frequency change.

Although the function f(E) in Equation 1 may be approximated by a mathematical function, it is of no particular advantage in a practical design. A graphical method is therefore used, and the steps of this are briefly outlined below.

FIG. 16

OSCILLATOR CIRCUIT FOR SINGLE VOLTAGE TRACKING

First, the capacity variation of the voltage sensitive capacitors is plotted as a function of applied voltage, E. A typical plot is shown in Figure 17a. In the particular circuit to be tuned, the capacitance of the coil, associated tube, and wiring is lumped together as C_s, and this value is added to C and the capacity variation replotted.

The second step in the graphical method is shown in Figure 17b. This is a plot of the frequency variation, and is obtained by plotting $k(C + C_s)^{-1/2}$ vs. E. The constant k is equal to $L^{-1/2}$.

It is now necessary to decide whether to sweep from high to low frequency or from low to high frequency. It is obvious that in sweeping from high to low the voltage E must change rapidly at first and slowly later. This suggests an electrical circuit with a negative exponent, which is readily realizable. There is an additional advantage in sweeping from the high frequency end to the low frequency. This is due to the fact that the flyback, or return sweep, is generally much faster than the main sweep, which allows considerably more time for discharge of the capacitors than for charging. Previous investigation[1] shows that the polarization lag, or response of the capacitor to changes in applied voltage, is more rapid on charge than on discharge.

The frequency limits f_2 and f_1 are noted on Figure 17b, and from these the required limits of voltage E_2 and E_1 are obtained. To obtain the required shape of voltage wave for linear frequency sweep, this curve is replotted in Figure 17c. Here, equal frequency intervals are replaced by equal time intervals along the baseline, and the solid curve shows the required voltage variation. It is generally possible to approximate this curve fairly closely by a single RC decay circuit as suggested by the simplified circuit to the right of the curve.

---

[1] See, for instance, Quarterly Progress Report No. 8, Task Order No. EDG-4, July 1953.

A. CAPACITY VARIATION

B. FREQUENCY VARIATION

C. SWEEP VOLTAGE FOR LINEAR FREQUENCY

FIG. 17

LINEARIZING THE FREQUENCY SWEEP

The time constant, R_1C_1, and the bias battery, E_b, may be adjusted to give the approximation indicated by the dashed curve.

3.5.4 Noise Figure Measurements. The method used in obtaining the noise figures of the F.E. units plus I.F. strip is described in this section.

After determining that the 2nd detector of the PANDU receiver was operating in the linear portion of its range during normal receiver operation, the test equipment was set up as shown in Figure 18. The scope was calibrated in

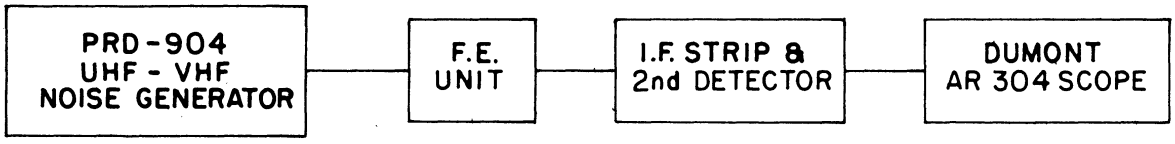

FIG. 18

TEST EQUIPMENT FOR NOISE FIGURE MEASUREMENTS

volts/inch of deflection on the "Y" axis and a convenient base line selected. With the dial of the Noise Generator set to zero (which terminates the line in its characteristic impedance), and the receiver operated under normal operating conditions, the dc voltage level due to the internal noise of the F.E. under test (plus IF strip) was measured from the base line. The noise figure (i.e., the noise power introduced at the receiver input terminals which causes the noise power at the 2nd detector to increase by a factor of 2 over that value obtained due to the internal noise alone) can be read directly in db from the dial plate of the noise generator. It should be noted that since the scope is a voltage measuring device, the dc level of noise voltage measured from the base line increases by a factor of approximately 1.4 as the noise power at the 2nd detector

is doubled.

It was found that the noise figure of the receiver using either FE-4 (28-76 mc) plus IF strip or FE-2 (68-130 mc) plus IF strip was approximately 19 db under sweeping conditions, and approximately 17 db under non-sweeping conditions.

The noise figure of the IF strip alone was approximately 11 db. However, the output of the PRD noise generator falls off below 30 mc; thus, the reliability of this figure is questionable.

Steps are now being taken to determine whether or not the internal noise of the IF strip contributes in any appreciable way to the overall noise figure of the receiver.

3.5.5 Measurements of Image Signal and Oscillator Second Harmonic Interference Effects. The image signal and the second harmonic of the oscillator can interact in the converter to produce interference with the desired signal. The following measurements were made with the receiver sweep voltage turned off.

The image signal sensitivity was found by adjusting the receiver tuning frequency to a convenient value, f_{s_1}, and then varying the signal generator carrier frequency over a range covering a frequency of $f_{s_1} + 2 f_i$, where f_i is the intermediate frequency. The carrier was modulated 30% and the carrier voltage was adjusted (when the frequency point of maximum audio output had been found) until a convenient power output level, P_1, was obtained. The modulated carrier of the signal generator was then set to the receiver tuning frequency, f_{s_1}, and the carrier was adjusted until the same power output level, P_1, attained with the image signal was again obtained. The same procedure was carried out with additional signal tuning frequencies f_{s_2}, f_{s_3}-f_{s_n}, and results were plotted as

$20 \log_{10} \frac{\text{image signal sensitivity}}{\text{real signal sensitivity}}$ against real signal frequency. Over the measurable range both FE-2 and FE-4 exhibited figures of approximately -30 to -35 db.

To determine the magnitude of oscillator second harmonic interference effects, the same test procedure as that described above can be used.

The oscillator second harmonic sensitivity was found by adjusting the receiver tuning frequency to a convenient value, f_{s_1}, and then varying the signal generator carrier frequency over a small range, which includes an undesired signal frequency spaced from the second harmonic of the oscillator by an amount equal to f_i (the intermediate frequency). The carrier was modulated 30% and the carrier voltage was adjusted (when the frequency point of maximum audio was found) until a convenient power output level, P_1, was obtained. The modulated carrier of the signal generator was then set to the receiver tuning frequency, f_{s_1}, and the carrier voltage was adjusted until the same power output level, P_1, was again obtained. The same procedure was carried out with the second harmonics of additional signal tuning frequencies f_{s_2}, f_{s_3} ... f_{s_n} and the results were plotted as $20 \log_{10} \frac{\text{oscillator 2nd harmonic sensitivity}}{\text{real signal sensitivity}}$ against real signal frequency. Over the range measured, which was just a mc or so at the extreme end of the band, FE-4 exhibited a figure of -50 to -55 db. The range of frequencies of the second harmonic of the oscillator in FE-2 was of such a high value (176-300 mc) that it would only mix with signals which were in the range 156-280 mc . Signals in this range were outside the pass band of the receiver and did not cause any interference.

4. CONCLUSIONS

The objectives for the period have been met, and all phases of the work appear to be progressing satisfactorily.

5. PROGRAM FOR NEXT INTERVAL

The program for the next interval will be concentrated primarily on the ferroelectric- and diode-tuning applications. A technical report containing all of the accumulated data on ferroelectric materials, in the form of ϵ-T-E surfaces, will be issued. Another technical report describing the details of construction of microcaps will be prepared. As a part of the materials and components program, the development of a suitable packaging for ferroelectric material will be re-examined, in conjunction with a study of the noise problem in dielectric amplifiers.

The PANDU program will be directed toward increasing the upper frequency of operation of electric tuned panoramic receivers, increasing the linearity of the frequency scan, and decreasing the noise figure by the use of low noise circuits.

DISTRIBUTION LIST

1 Copy	Director, Electronic Research Laboratory Stanford University Stanford, California Attn: Dean Fred Terman
1 Copy	Commanding General Army Electronic Proving Ground Fort Huachuca, Arizona Attn: Director, Electronic Warfare Department
1 Copy	Chief, Research and Development Division Office of the Chief Signal Officer Department of the Army Washington 25 D. C. Attn: SIGEB
1 Copy	Chief, Plans and Operations Division Office of the Chief Signal Officer Washington 25, D. C. Attn: SIGEW
1 Copy	Countermeasures Laboratory Gilfillan Brothers, Inc. 1815 Venice Blvd. Los Angeles 6, California
1 Copy	Commanding Officer White Sands Signal Corps Agency White Sands Proving Ground Las Cruces, New Mexico Attn: SIGWS-CM
1 Copy	Commanding Officer Signal Corps Electronics Research Unit 9560th TSU Mountain View, California
60 Copies	Transportation Officer, SCEL Evans Signal Laboratory Building No. 42, Belmar, New Jersey FOR - SCEL Accountable Officer Inspect at Destination File No. 22824-PH-54-91(1701)
1 Copy	J. A. Boyd Engineering Research Institute University of Michigan Ann Arbor, Michigan

1 Copy	H. W. Welch, Jr. Engineering Research Institute University of Michigan Ann Arbor, Michigan
1 Copy	Document Room Willow Run Research Center University of Michigan Willow Run, Michigan
10 Copies	Electronic Defense Group Project File University of Michigan Ann Arbor, Michigan
1 Copy	Engineering Research Institute Project File University of Michigan Ann Arbor, Michigan